



DOI: 10.22363/2312-8143-2023-24-1-86-94

EDN: EEDRTQ

UDC 550.8+550.4+550.3

Research article / Научная статья

## Geochemical features of granitic rocks using x-ray spectral fluorescence in the Miass region, Southern Ural

Mohammed Abdalla Elsharif Ibrahim<sup>a</sup> , Vladimir N. Kuleshov<sup>b</sup> , Alexander E. Kotelnikov<sup>a</sup> ,  
Alexey F. Georgievskiy<sup>a</sup> , Samia Abdelrahman Ibrahim<sup>c</sup>

<sup>a</sup> RUDN University, Moscow, Russian Federation

<sup>b</sup>Geological Institute of the Russian Academy of Sciences, Moscow, Russian Federation

<sup>c</sup>University of Khartoum, Khartoum, Republic of Sudan

[mohammedelsharif7@gmail.com](mailto:mohammedelsharif7@gmail.com)

### Article history

Received: December 14, 2022

Revised: February 25, 2023

Accepted: February 28, 2023

### Keywords:

geochemistry, magma process, high-K calc-alkaline, metaluminous

**Abstract.** The goals of the research are the geochemistry and identification of granite rocks. The granitic rocks are part of the Syrostan massive, which is located in Southern Ural. Understanding the magma process and probable mineralization deposition can be gained by classifying granite and determining geochemical characteristics. X-ray spectral fluorescence analysis was used to collect samples from outcrops for geochemical analysis. The results indicate that the rocks belong to the high-K calc-alkaline to calc-alkaline series. The granites are metaluminous to slightly peraluminous and are classified as I-type granites, with A/CNK values ranging from 0.73 to 1.01. The majority of the rock samples are trondhjemite to slightly tonalite in composition. The most observable samples in the normative Na<sub>2</sub>O-k<sub>2</sub>O-CaO scheme have defined a continuous range, varying from tonalite/trondhjemite to granodiorite. The findings provide valuable information about the petrogenesis of the rocks and their composition.

### Acknowledgements

This paper has been supported by the RUDN University Strategic Academic Leadership Program.

### Conflicts of interest

The authors declare that they have no known competing financial interests or personal relationships that could have appeared to influence the study presented in the paper.

### For citation

Ibrahim MAE, Kuleshov VN, Kotelnikov AE, Georgievskiy AF, Ibrahim SA. Geochemical features of granitic rocks using x-ray spectral fluorescence in the Miass region, Southern Ural. *RUDN Journal of Engineering Research*. 2023;24(1):86–94.  
<http://doi.org/10.22363/2312-8143-2023-24-1-86-94>

## Геохимическая характеристика и классификация гранитов с использованием рентгеновской спектральной флуоресценции Миасского района Южного Урала

М.А.А. Ибрахим<sup>a</sup>, В.Н. Кулешов<sup>b</sup>, А.Е. Котельников<sup>a</sup>,  
А.Ф. Георгиевский<sup>a</sup>, С.А. Ибрахим<sup>c</sup>

<sup>a</sup>Российский университет дружбы народов, Москва, Российская Федерация

<sup>b</sup>Геологический институт Российской академии наук, Москва, Российская Федерация

<sup>c</sup>Университет Хартума, Хартум, Республика Судан

 mohammedelsharif7@gmail.com

### История статьи

Поступила в редакцию: 14 декабря 2022 г.  
Доработана: 25 февраля 2023 г.  
Принята к публикации: 28 февраля 2023 г.

### Ключевые слова:

геохимия, рентгеноспектральная  
флуоресценция, магматический процесс,  
высококалиевый, известково-щелочной,  
металлургический

**Аннотация.** Основные задачи исследования – геохимия и идентификация гранитных пород. Гранитные породы входят в состав Сыростанского массива, расположенного на Южном Урале. Понимание магматического процесса и вероятного отложения минерализации можно получить путем классификации гранита и определения геохимических характеристик. Рентгеноспектральный флуоресцентный анализ использован для отбора проб из обнажений для геохимического анализа. Результаты показали, что породы относятся к известково-щелочной серии. Граниты – от металлюминозных до слабоглиноземистых – относятся к I типу со значениями A/CNK от 0,73 до 1,01. Большинство образцов пород имеют состав от трондьемита до слабого тоналита. Наиболее наблюдаемые образцы в нормативной схеме  $\text{Na}_2\text{O}$ - $\text{K}_2\text{O}$ - $\text{CaO}$  определяют непрерывный диапазон от тоналита/трондьемита до гранодиорита. Найдки дают ценную информацию о петрогенезе горных пород и их составе.

### Благодарности

Работа выполнена при поддержке Программы стратегического академического лидерства РУДН.

### Заявление о конфликте интересов

Авторы заявляют, что им неизвестны конкурирующие финансовые интересы или личные отношения, которые могли бы повлиять на представленное в статье исследование.

### Для цитирования

Ibrahim M.A.E., Kuleshov V.N., Kotelnikov A.E., Georgievskiy A.F., Ibrahim S.A. Geochemical features of granitic rocks using x-ray spectral fluorescence in the Miass region, Southern Ural // Вестник Российского университета дружбы народов. Серия: Инженерные исследования. 2023. Т. 24. № 1. С. 86–94. <http://doi.org/10.22363/2312-8143-2023-24-1-86-94>

### Introduction

Different deposits and mineralization were discovered associated with granite intrusions, such as gold deposits, tin, tungsten and several deposits of rare earth elements [1; 2]. Type, origin, and petrogenesis of granite is significant key in formation of specific deposits. Some studies revealed that, various of rare earth elements deposits related to highly fractionated granite intrusions. Also, the Syrostan massive in the southern Ural linked with many deposits such as gold, rare earth elements, and skarn deposits. Therefore, determine the type of granite, identification the magma evolution process, and the geochemistry of granite could lead to a potential ore deposit.

Although, several research were conducted in the Syrostan massive and intrusions in southern Ural looking for potential mineralization [2–6]; however, the massive area was not covered with the investigation of the petrogenesis and the geochemistry and conducted them to the mineralization. The aim of this study is to identify geochemical characteristic and type of the granite in order to connect them with type of mineralization and use the result for future researches.

*Geology of the study area.* The Syrostan massive locates in the southwest of the Miass city, southern Ural in the zone of the main Ural deep fault. The massive is among metabasites, shales of several composition and fragment of metamor-

phosed oceanic crust and the crust of passive margin of the Ural paleocean. The massive is formed in the lower carbonian and has three phases: the first is granodiorite and quartz diorite, the second is double feldspar and plagiogranite, and the third is vein complex [6–8].

The location of the study area almost 15 km northwest of the Miass city (Figure 1). The area of

the massive consists of metamorphic complex and marble body lies in the form of lenses crossed by several granite veins and the marble mainly in contact with diorite. The magmatic complex includes quartz diorite, granodiorite, biotite granite, and leucogranite [6; 9; 10]. After intensive of petrographic investigation, nine samples have been selected for major oxides analysis.

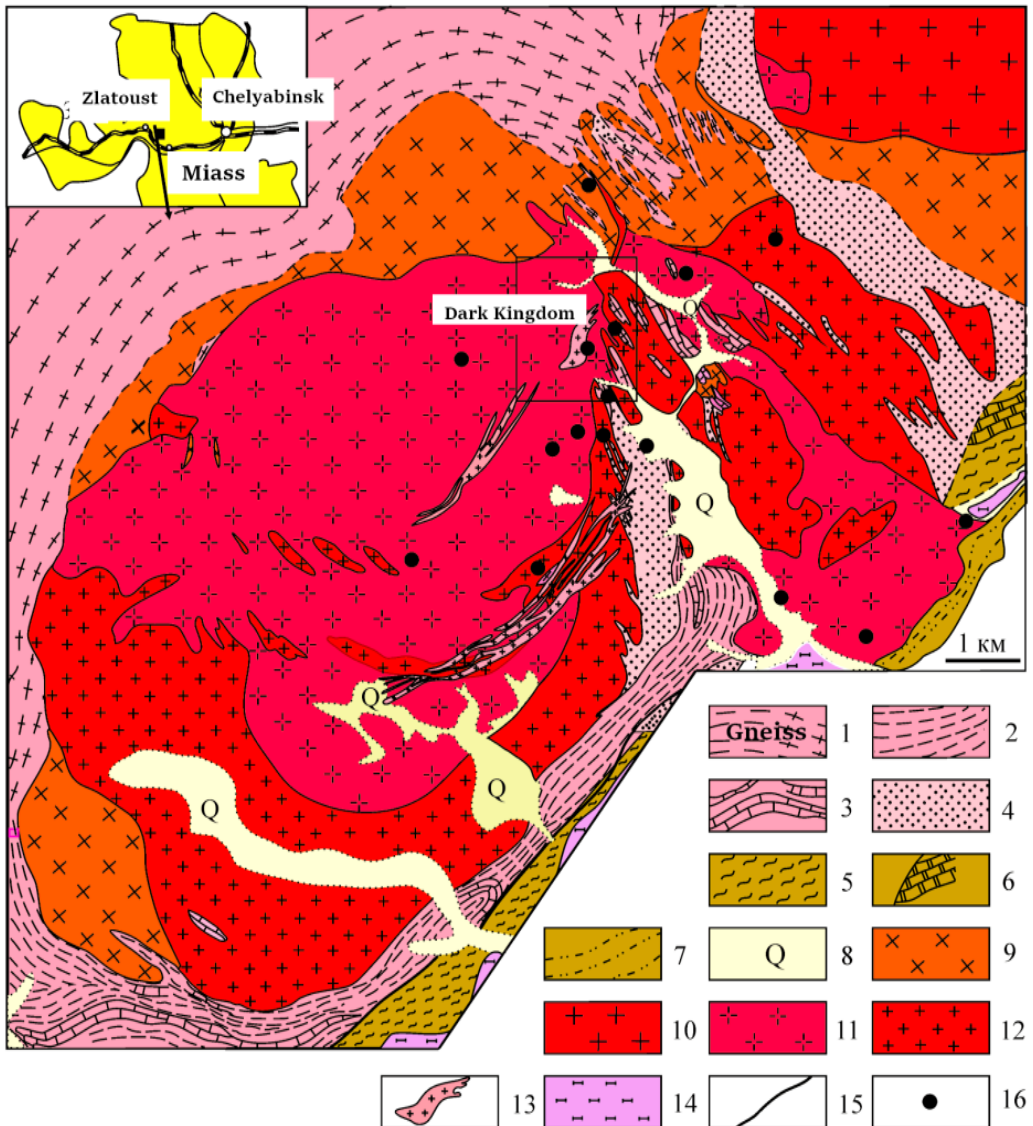


**Figure 1.** The Syrostan granite massive's modified geological map, which includes the Dark Kingdom of Marble Deposit:  
1 – gneiss; 2 – mica quartz schist; 3 – marble limestone; 4 – quartzite; 5 – shale; 6 – marble; 7 – carbonaceous shale;  
8 – quaternary sediments; 9 – granodiorite, quartz diorite, diorite; 10 – porphyric biotite granites; 11 – pink porphyric biotite granites;  
12 – veined granite and plagiogranite; 13 – pegmatites; 14 – serpentinites; 15 – tectonic faults; 16 – occurrence of niobium

## 1. Analytical methods

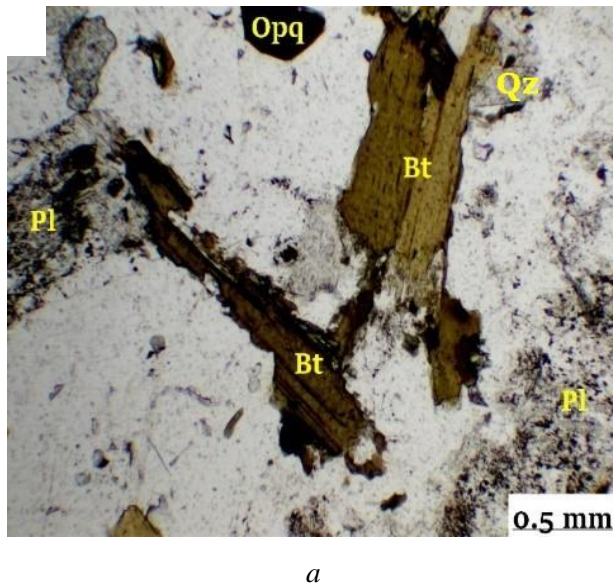
Determination of the concentration of major oxides in the samples was executed by x-ray spectral fluorescence analysis (XRF) on a sequential vacuum

spectrometer (with wavelength dispersion), model Axios mAX manufactured by PAN analytical (Netherlands). The analysis was performed at the Center for Collective Use of the IGEM RAS (Moscow, Russia).

## 2. Results and discussion

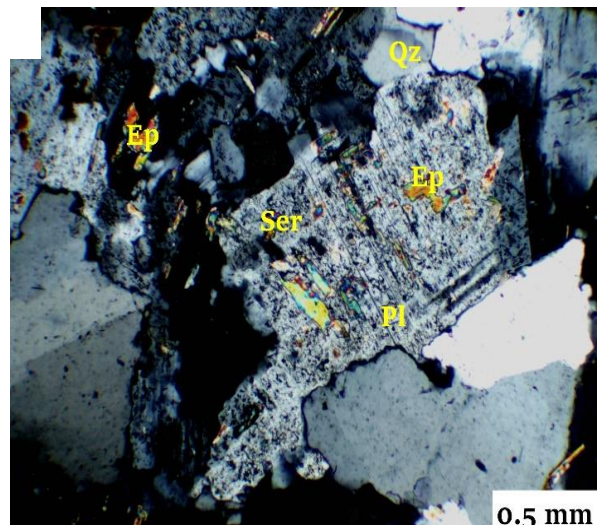
### 2.1. Petrography and mineral compositions

Microgranite is composed primarily of quartz (15–25%), microcline (20–50%), plagioclase (20–40%), and biotite (5–10%) and has a medium to coarse grained texture (Figure 2, *a*). Recrystallized quartz has two generations. This indicates that there



*a*

has been deformation. Sericite and muscovite are discovered after plagioclase. Plagioclase exhibits sericitization and epidotization as a result of hydrothermal activity [11; 12]. Plagioclase zoning shows epidote and sericite from core to rim (Figure 2, *b*). Furthermore, chlorite, epidote, and calcite are secondary minerals. Accessory minerals include opaque minerals such as zircon and apatite.



*b*

**Figure 2.** A microscopic examination of granitic and diorite rocks:  
*a* – granitic rocks with quartz, plagioclase, and biotite (analyzer out);  
*b* – plagioclase grain partially mixed with a sericite aggregate (analyzer in)

### 2.2. Geochemical properties and granitic rocks types

Table 1 shows the major oxides and geochemical compositions of granitoids rocks. Classification of granitoids rocks using TAS diagram [13] shows that most rocks are granite and one sample is syenodiorite (Figure 3, *a*), similarly the classification based on Middlemost diagram [14], total alkali vs. silica demonstrate the rocks as granite, monzodiorite, and monzonite (Figure 3, *b*). The investigated granite samples have a high SiO<sub>2</sub> contents ranging from 76.15 to 59.55 wt.%.

Diorite shows and silica content about (52.9 wt.%). Granite samples have high total alkalis K<sub>2</sub>O + Na<sub>2</sub>O ranging between (7–10 wt.%), moderate K<sub>2</sub>O/Na<sub>2</sub>O ratios ranging from 0.35 to 0.85, and low to intermediate CaO (0.5 to 6 wt.%), that followed by low content of P<sub>2</sub>O<sub>5</sub> (0.01 to 0.5%). The LOI (loss on ignition) values ranging from 0.6 to 2 wt.% which is reflect low value. On the K<sub>2</sub>O with SiO<sub>2</sub> diagram [15], the investigated samples fall into the

high-K calc-alkaline series to slightly calc alkaline series (Figure 3, *c*).

Similarly, the AFM diagram (A = K<sub>2</sub>O + Na<sub>2</sub>O, F = FeOt, and M = MgO) [16], demonstrates the evolution of magma form tholeiite into calc alkaline series (Figure 3, *d*).

Al saturation index A/CNK molar (Al<sub>2</sub>O<sub>3</sub>/CaO + Na<sub>2</sub>O + K<sub>2</sub>O) vs. A/NK molar (Al<sub>2</sub>O<sub>3</sub>/Na<sub>2</sub>O + K<sub>2</sub>O) diagram is plotted and shows the samples plot within the metaluminous field to slightly peraluminous (Figure 3, *e*) based on the SiO<sub>2</sub> vs. FeOt/(FeOt + MgO) diagram (Figure 3, *f*), determine the samples are magnesian. Both diagrams indicate the type of granite as I-type granite which is related to igneous origin and absence of involving of sedimentary materials.

The result of CIPW norm present in Table 2, norm of granite shows quartz ranging from 5 to 30 wt.%, that indicates the granite standard. The investigated samples have a high albite with values ranging from 37.5 to 50.5 wt.%, and mode-

rate orthoclase content, with values ranging between, 14.5 to 21.5 wt.%. The norm of corundum in most sample shows 0 value and the rest of samples shows values less than 1 in the average of 0.5 wt.%. These result implying, I-type granite [17; 18]. Using

the normative result with more than 10% of Quartz, Ab-An-Or diagram has been plotted (Figure 4, a). the diagram shows the trondhjemite as dominant plutonic rock type, granite and tonalite represent the rest of the samples.

Table 1

**Compositions of whole rock major oxides in granitoid rocks**

Major oxides, wt. %	Samples								
	MG1	MG2	MG3	LG1	LG2	LG3	BG1	BG3	D1
SiO <sub>2</sub>	70.64	70.45	69.85	73.43	76.17	74.62	69.52	59.54	52.89
Al <sub>2</sub> O <sub>3</sub>	14.62	15.17	14.82	12.71	12.89	13.84	15.38	17.3	17.95
Na <sub>2</sub> O	5.29	4.89	4.94	5.98	5.84	5.63	4.42	5.33	5.34
MgO	0.53	0.46	0.75	0.19	0.1	0.08	0.82	1.65	3.95
K <sub>2</sub> O	3.47	3.43	3.45	2.44	2.47	3.61	3.67	3.5	2
CaO	2.06	1.81	1.99	2.77	0.95	0.53	2.23	4.81	6.37
TiO <sub>2</sub>	0.23	0.22	0.21	0.02	0.03	0.02	0.39	0.66	1.18
MnO	0.043	0.037	0.038	0.015	0.022	0.007	0.033	0.093	0.096
Fe <sub>2</sub> O <sub>3</sub>	1.93	1.82	1.98	0.28	0.52	0.36	2.51	5.02	7.61
P <sub>2</sub> O <sub>5</sub>	0.09	0.07	0.07	0.01	0.02	0.02	0.14	0.28	0.53
LOI	0.81	1.19	1.58	2.13	0.83	1.13	0.64	1.34	1.08
SUM	99.71	99.55	99.68	99.98	99.84	99.85	99.75	99.52	98.99
A/NK	1.17	1.29	1.25	1.02	1.05	1.05	1.37	1.38	1.64
A/CNK	0.902	1.01	0.957	0.725	0.92	0.979	1.005	0.812	0.796
K <sub>2</sub> O/Na <sub>2</sub> O	0.655	0.701	0.698	0.408	0.422	0.641	0.83	0.656	0.374
Na <sub>2</sub> O/K <sub>2</sub> O	1.52	1.43	1.42	2.45	2.36	1.56	1.2	1.52	2.67

Table 2

**CIWP norm for investigated samples**

Mineral, wt. %	Samples								
	MG1	MG2	MG3	LG1	LG2	LG3	BG1	BG3	D1
Quartz	22.45	24.5	23.05	25.95	31.25	27.01	24.15	5.15	0
Corundum	0	0.23	0	0	0	0	0.5	0	0
Orthoclase	20.5	20.3	20.5	14.5	14.5	21.5	21.5	20.6	11.8
Albite	44.7	41.5	41.8	50.5	49.5	47.6	37.4	45.1	45.2
Anorthite	5.8	8.5	8	0.63	1.66	1.83	10.15	12.94	19.10
Diopside	2.4	0	0.59	1.02	0.53	0.43	0	5.57	3.85
Wollastonite	0	0	0	4.89	0.92	0.03	0	0	0
Hypersthene	0.2	1.14	1.594	0	0	0	2.04	1.53	1.67
Olivine	0	0	0	0	0	0	0	0	4.47
Ilmenite	0.09	0.07	0.08	0.03	0.04	0.02	0.071	0.3	0
Hematite	1.9	1.82	1.98	0.28	0.52	0.36	2.51	5.02	7.6
Sphene	0.5	0	0.41	0.008	0.02	0.03	0	1.4	2.89
Rutile	0	0.17	0	0	0	0	0.35	0	0
Apatite	0.2	0.16	0.16	0.02	0.05	0.05	0.33	0.66	1.25
Pyrite	0	0	0	0	0	0	0	0	0.16
Sum	98.9	98.4	98.11	97.85	99.02	98.73	99.13	98.20	98.02

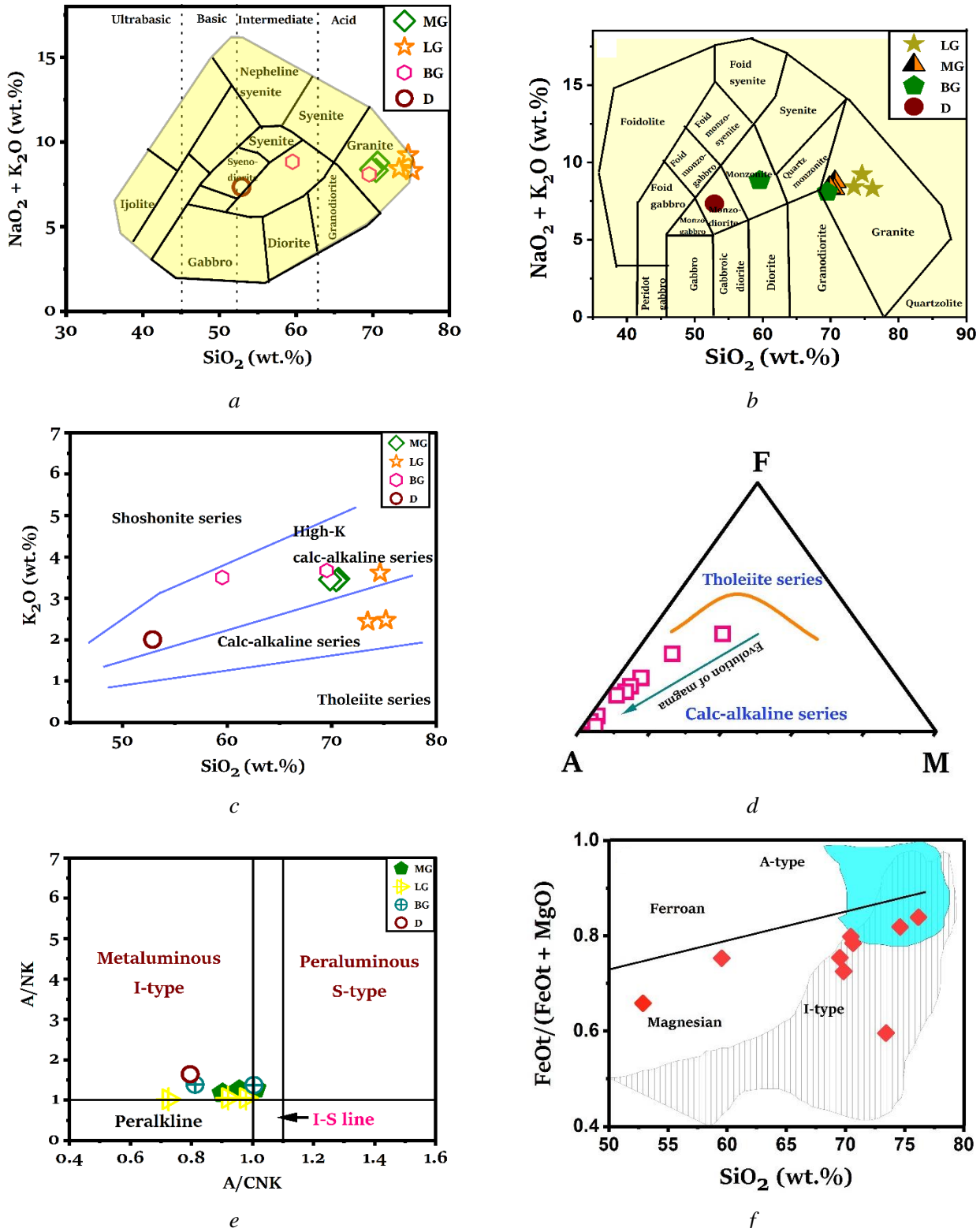


**Figure 3.** Plots and classification of the Miass granitoid's major oxides:

a – total alkali silica of plutonic rocks [13]; b – TAS diagram for granitoid classification [14];

c –  $\text{SiO}_2$  versus  $\text{K}_2\text{O}$  diagram [15], showing the presence of granitoid rocks among the high-K calc-alkaline series;

d – AFM diagram with  $A = (\text{K}_2\text{O} + \text{Na}_2\text{O})$ ,  $F = \text{FeOt}$ , and  $M = \text{MgO}$  [16], showing rock samples from the calc-alkaline series with high  $\text{K}_2\text{O} + \text{Na}_2\text{O}$ ;

e – Al saturation index  $A/\text{CNK}$  molar [ $\text{Al}_2\text{O}_3/(\text{CaO}+\text{Na}_2\text{O}+\text{K}_2\text{O})$ ] versus  $A/\text{NK}$  molar [ $\text{Al}_2\text{O}_3/(\text{Na}_2\text{O}+\text{K}_2\text{O})$ ] diagram, indicating metaluminous to peraluminous samples;

f – as a result of the  $\text{SiO}_2$  vs  $\text{FeOt}/(\text{FeOt} + \text{MgO})$  diagram, all of the samples are magnesian

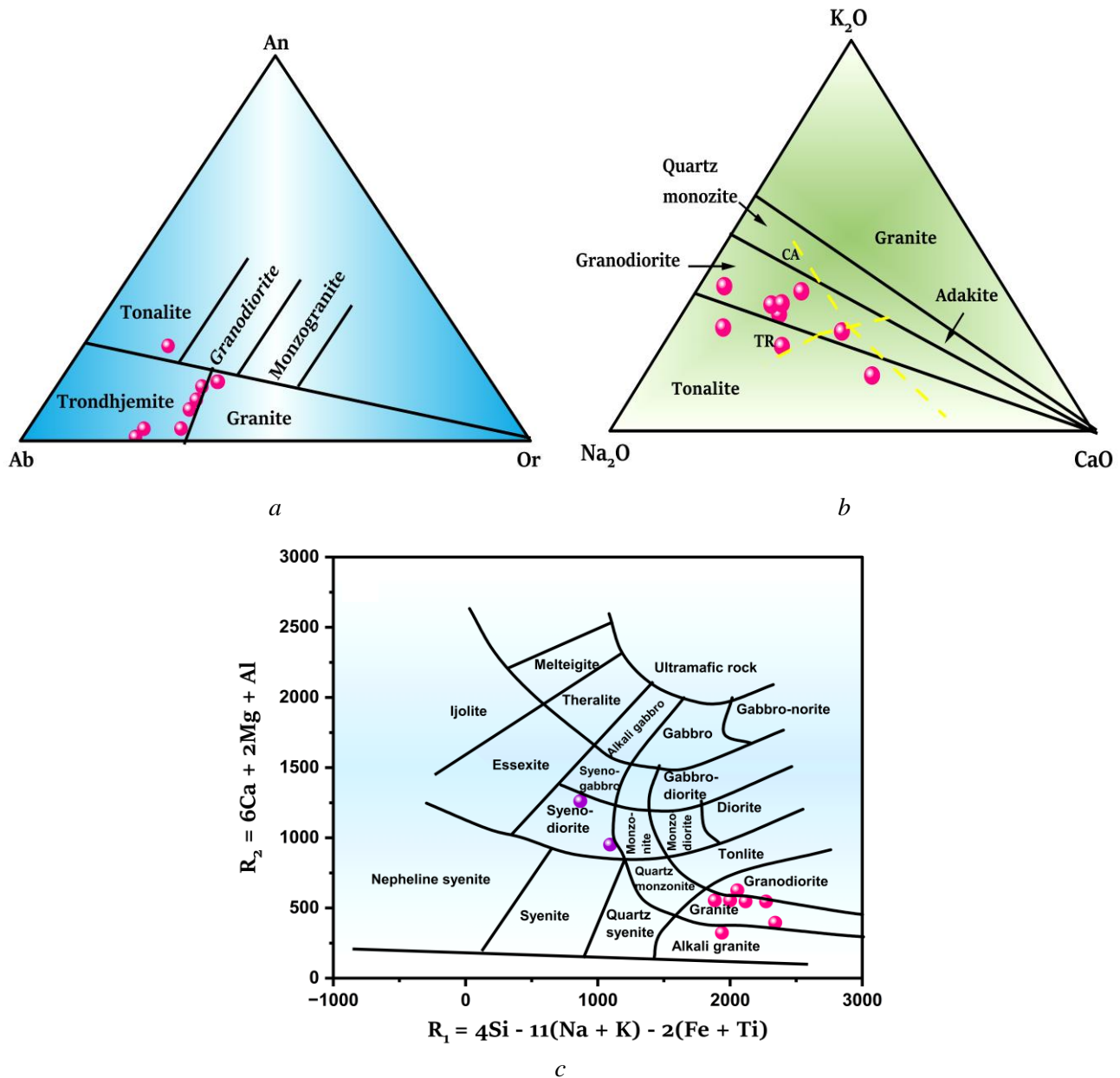


**Figure 4.** Classifying the igneous rocks using the norm and cations:  
 a – normative Ab-An-Or ternary plot and classification of rocks in the study area using Barker's scheme (1979) [20];  
 b – Na<sub>2</sub>O-K<sub>2</sub>O-CaO ternary plot for Southern Ural studied rocks,  
 Barker's (1979) [20], calc-alkaline (CA) and trondhjemite (TR) differentiation trends are represented by dashed curves;  
 c – the classification of plutonic rocks using the parameter R1 & R2 after [19] calculated from millications proportions,  
 $R1 = 4Si - 11(Na + K) - 2(Fe + Ti)$ ,  $R2 = (Al + 2Mg + 6Ca)$

On Na<sub>2</sub>O-K<sub>2</sub>O-CaO diagram (Figure 4, b) define a continuous range from tonalite/trondhjemite to granodiorite as the most observable samples.

Using the categorization diagram (Figure 4, c) from [19], for plutonic igneous rocks based on their millications or cation proportions, that widely use and more accurate in classification of plutonic rocks. The plotting parameters RI and R2 are used

to plot the data on an x-y bivariate graph. R1 is defined as [4Si – 11(Na + K) – 2(Fe + Ti)] and is displayed on the r-axis. Fe stands for total iron. R2 is shown as a plot along the y-axis and has the formula R2 = (Al + 2Mg + 6Ca). The samples define a continuous range from granite to alkali granite, granodiorite, and syenodiorite, with granite being the most common.

## Conclusion

Granite is silica-enriched with  $\text{SiO}_2$  ranging between (~76.14–59.54 wt.%) however, diorite shows intermediate chemical composition of  $\text{SiO}_2$  (~52.89 wt.%). The studied samples show high total alkalis  $\text{K}_2\text{O} + \text{Na}_2\text{O} = (7.34\text{--}9.24 \text{ wt.}\%)$ ,  $\text{K}_2\text{O}/\text{Na}_2\text{O}$  display moderate ratios ranging from (~0.83–0.37). Low  $\text{CaO}$  (0.53–6.37 wt.%), and  $\text{P}_2\text{O}_5$  (0.01–0.53 wt.%) contents. The rocks belong to the high-K calc-alkaline series to slightly calc alkaline series, and they are metaluminous.

The results show that the majority of the rock samples are classified as trondhjemite to slightly tonalite. The samples in the normative  $\text{Na}_2\text{O}-\text{K}_2\text{O}-\text{CaO}$  have defined a continuous range as the most observable samples, ranging from tonalite/trondhjemite to granodiorite.

The petrography investigation of this study revealed ore minerals and indications of hydrothermal solution suggesting mineralization process. The massive associated with many deposits and mineralization such as gold, skarn, and rare earth deposits.

## References

1. Xie L, Liu Y, Wang R, Hu H, Che X, Xiang L. Li–Nb–Ta mineralization in the Jurassic Yifeng granite aplite intrusion within the Neoproterozoic Jiuling batholith, South China: a fluid-rich and quenching ore-forming process. *Journal of Asian Earth Sciences*. 2019;185:104047. <https://doi.org/10.1016/j.jseas.2019.104047>
2. Makagonov EP, Muftahov VA. Rare-earth and rare-metal mineralization in late granite of Syrostan massif (Southern Urals). *Lithosphere (Russia)*. 2015;(2):121–132. (In Russ.)  
Макагонов Е.П., Муфтахов В.А. Редкоземельно-редкометалльная минерализация в поздних гранитах Сыростанского массива (Южный Урал) // Литосфера. 2015. № 2. С. 121–132.
3. Fershtater GB, Krasnobaev AA, Bea F, Montero P, Borodina NS. Geodynamic settings and history of the Paleozoic intrusive magmatism of the central and southern Urals: results of zircon dating. *Geotectonics*. 2007;41(6):465–486. <https://doi.org/10.1134/S0016852107060039>
4. Kholodnov VV, Shardakova GYu, Puchkov VN, Petrov GA, Shagalov E, Salikhov DN, Korovko AV, Pribavkin SV, Rakhimov I, Borodina NS. Paleozoic granitoid magmatism of the Urals: the reflection of the stages of the geodynamic and geochemical evolution of a collisional orogen. *Geodynamics & Tectonophysics*. 2021;12(2):225–245. <https://doi.org/10.5800/GT-2021-12-2-0522>
5. Fershtater GB, Borodina NS, Bea F, Montero P. Model of mantle-crust interaction and magma generation in the suprasubduction orogen (Paleozoic of the Urals). *Lithosphere (Russia)*. 2018;18(2):177–207. (In Russ.) <https://doi.org/10.24930/1681-9004-2018-18-2-177-207>
- Ферштатер Г.Б., Бородина Н.С., Беа Ф., Монтеро П. Модель мантийно-корового взаимодействия и сопряженного магматизма в надсубдукционном орогене (палеозой Урала) // Литосфера. 2018. Т. 18. № 2. С. 121–132. <https://doi.org/10.24930/1681-9004-2018-18-2-177-207>
6. Georgievskiy AF, Bugina VM, Kotelnikov AE, Georgievskiy AA, Mahinja E, Gamilton ZA, Vein-rock in the Dark Kingdom Marble Deposit (South Ural) and their possible connection with gold ore mineralization. *IOP Conference Series: Earth and Environmental Science*. 2021;666(2):022024. <https://doi.org/10.1088/1755-1315/666/2/022024>
7. Bea F, Fershtater GB, Montero P, Smirnov VN, Molina JF. Deformation-driven differentiation of granitic magma: the Stepninsk pluton of the Uralides, Russia. *Lithos*. 2005;81(1–4):209–233. <https://doi.org/10.1016/j.lithos.2004.10.004>
8. Salikhov DN, Kholodnov VV, Puchkov VN, Rakhimov IR. Volcanism and intrusive magmatism of the Magnitogorsk paleoarc in the epoch of its ‘soft’ collision with a margin of the east European continent. *Lithosphere (Russia)*. 2020;20(5):630–651. (In Russ.) <https://doi.org/10.24930/1681-9004-2020-20-5-630-651>
- Салихов Д.Н., Холоднов В.В., Пучков В.Н., Рахимов И.Р. Вулканизм и интрузивный магматизм Магнитогорской палеодуги в эпоху «мягкой» коллизии с окраиной Восточно-Европейского континента // Литосфера. 2020. Т. 20. № 5. С. 630–651. <https://doi.org/10.24930/1681-9004-2020-20-5-630-651>
9. Scarrow JH, Ayala C, Kimbell GS. Insights into orogenesis: getting to the root of a continent-ocean-continent collision, Southern Urals, Russia. *Journal of the Geological Society*. 2002;159(6):659–671. <https://doi.org/10.1144/0016-764901-147>
10. Stadtlander R, Mechle J, Schulze A. Deep structure of the Southern Ural mountains as derived from wide-angle seismic data. *Geophysical Journal International*. 1999;137(2):501–515. <https://doi.org/10.1046/j.1365-246X.1999.00794.x>
11. Pittarello L, Levi N, Wegner W, Stehlik H. The pseudotachylites at the base of the Silvretta Nappe: a newly discovered recent generation and the tectonometamorphic evolution of the Nappe. *Tectonophysics*. 2022;822:229185. <https://doi.org/10.1016/j.tecto.2021.229185>
12. Chen Y, Niu Y, Shen F, Gao Y, Wang X. New U-Pb zircon age and petrogenesis of the plagiogranite, Troodos ophiolite, Cyprus. *Lithos*. 2020;362–363:10547. <https://doi.org/10.1016/j.lithos.2020.105472>
13. Cox KG, Bell JD, Pankhurst RJ. Quaternary systems. *The Interpretation of Igneous Rocks*. Dordrecht: Springer; 1979. p. 197–221. [https://doi.org/10.1007/978-94-017-3373-1\\_8](https://doi.org/10.1007/978-94-017-3373-1_8)

14. Middlemost EAK. Naming materials in the magma/igneous rock system. *Earth-Science Reviews*. 1994;37(3–4): 215–224. [https://doi.org/10.1016/0012-8252\(94\)90029-9](https://doi.org/10.1016/0012-8252(94)90029-9)
15. Peccerillo A, Taylor SR. Geochemistry of eocene calc-alkaline volcanic rocks from the Kastamonu area, Northern Turkey. *Contributions to Mineralogy and Petrology*. 1976;58(1):63–81. <https://doi.org/10.1007/BF00384745>
16. Irvine TN, Baragar WRA. A guide to the chemical classification of the common volcanic rocks. *Canadian Journal Earth Sciences*. 1971;8(5):523–548. <https://doi.org/10.1139/e71-055>
17. Ahnaf JS, Patonah A, Permana H. Petrogenesis of volcanic arc granites from Bayah complex, Banten, Indonesia. *Journal of Geoscience, Engineering, Environment, and Technology*. 2019;4(2):3171. <https://doi.org/10.25299/jgeet.2019.4.2.3171>
18. Chappell BW, Bryant CJ, Wyborn D. Lithos peraluminous I-type granites. *Lithos*. 2012;153:142–153. <https://doi.org/10.1016/j.lithos.2012.07.008>
19. De la Roche H, Leterrier J, Grandclaude P, Marchal M. A classification of volcanic and plutonic rocks using R1R2-diagram and major-element analyses – its relationships with current nomenclature. *Chemical Geology*. 1980;29(1–4): 183–210. [https://doi.org/10.1016/0009-2541\(80\)90020-0](https://doi.org/10.1016/0009-2541(80)90020-0)
20. Barker F. Chapter 1 – Trondhjemite: definition, environment and hypotheses of origin. *Developments in Petrology*. 1979;6:1–12. <https://doi.org/10.1016/B978-0-444-41765-7.50006-X>

## About the authors

**Mohammed Abdalla Elsharif Ibrahim**, PhD student, Department of Mineral Development and Oil & Gas Engineering, Academy of Engineering, RUDN University, 6 Miklukho-Maklaya St, Moscow, 117198, Russian Federation; ORCID: 0000-0002-5634-5695, Scopus Author ID: 57200327978, eLIBRARY SPIN-code: 8757-5907; mohammedel-sharif7@gmail.com

**Vladimir N. Kuleshov**, Doctor of Sciences (Geochemistry), chief researcher, Geological Institute, Russian Academy of Sciences, 7 Pyzhevskii Pereulok, Moscow, 119017, Russian Federation; ORCID: 0000-0003-4925-5154, Scopus Author ID: 8073984000, eLIBRARY SPIN-code: 5867-2758; vnkuleshov@mail.ru

**Alexander E. Kotelnikov**, PhD in Geology, Associate Professor, Head of the Department of Mineral Development and Oil & Gas Engineering, Academy of Engineering, RUDN University, 6 Miklukho-Maklaya St, Moscow, 117198, Russian Federation; ORCID: 0000-0003-0622-8391, Scopus Author ID: 57205586833, Researcher ID: O-3821-2019, eLIBRARY SPIN-code: 6280-5070; kotelnikov-ae@rudn.ru

**Alexey F. Georgievskiy**, Doctor of Sciences (Geological and Mineralogical), Associate Professor of the Department of Mineral Development and Oil & Gas Engineering, Academy of Engineering, RUDN University, 6 Miklukho-Maklaya St, Moscow, 117198, Russian Federation; ORCID: 0000-0003-4835-760X, Scopus Author ID: 57212305311, eLIBRARY SPIN-code: 1308-9195; georgievskiy-af@rudn.ru

**Samia Abdelrahman Ibrahim**, PhD in Geology, Head of the Department of Geology, Faculty of Science, University of Khartoum, Al-Gama'a Avenue, Khartoum, 11111, Republic of Sudan; samiaibrahim125@gmail.com

## Сведения об авторах

**Ибрахим Мухаммед Абдалла Альшариф**, аспирант, департамент недропользования и нефтегазового дела, Инженерная академия, Российский университет дружбы народов, Российская Федерация, 117198, Москва, ул. Миклухо-Маклая, д. 6; ORCID: 0000-0002-5634-5695, Scopus Author ID: 57200327978, eLIBRARY SPIN-код: 8757-5907; mohammedelsharif7@gmail.com

**Кулешиов Владимир Николаевич**, доктор геолого-минералогических наук, главный научный сотрудник, Геологический институт, Российской академии наук, Российской Федерации, 119017, Пыжевский пер., д. 7; ORCID: 0000-0003-4925-5154, eLIBRARY SPIN-код: 5867-2758; vnkuleshov@mail.ru

**Котельников Александр Евгеньевич**, кандидат геолого-минералогических наук, доцент, директор департамента недропользования и нефтегазового дела, Инженерная академия, Российский университет дружбы народов, Российской Федерации, 117198, Москва, ул. Миклухо-Маклая, д. 6; ORCID: 0000-0003-0622-8391, Scopus Author ID: 57205586833, Researcher ID: O-3821-2019, eLIBRARY SPIN-код: 6280-5070; kotelnikov-ae@rudn.ru

**Георгиевский Алексей Федорович**, доктор геолого-минералогических наук, доцент департамента недропользования и нефтегазового дела, Инженерная академия, Российский университет дружбы народов, Российской Федерации, 117198, Москва, ул. Миклухо-Маклая, д. 6; ORCID: 0000-0003-4835-760X, Scopus Author ID: 57212305311, eLIBRARY SPIN-код: 1308-9195; georgievskiy-af@rudn.ru

**Ибрахим Самия Абдельрахман**, кандидат геологических наук, директор департамента геологии, факультет естественных наук, Хартумский университет, Республика Судан, 11111, Хартум, пр-кт Аль-Гамаа; samiaibrahim125@gmail.com